Editors' choice

3D analyses of the first ortholasmatine harvestmen from European Eocene ambers

CHRISTIAN BARTEL, PLAMEN G. MITOV, JASON A. DUNLOP, and JÖRG U. HAMMEL

Bartel, C., Mitov, P.G., Dunlop, J.A., and Hammel, J.U. 2026. 3D analyses of the first ortholasmatine harvestmen from European Eocene ambers. *Acta Palaeontologica Polonica* 71 (1): 95–107.

The first fossil representatives of the harvestman subfamily Ortholasmatinae (Opiliones, Dyspnoi, Nemastomatidae) are described as *Balticolasma wunderlichi* gen. et sp. nov. One male is preserved in Eocene Baltic amber and a presumably conspecific female in Eocene Rovno amber (northwest Ukraine). Ortholasmatines are typically highly ornate arachnids, and for the first time with an amber harvestman we applied computed tomography using synchrotron radiation to investigate its three-dimensional morphology and surface structure in considerable detail. Some of its morphological characters, appear to be closer to extant Asian genera. In a wider biogeographic context, our amber record is a significant find for the Paleogene of Europe given that (i) it is another species apparently found in both Baltic and Rovno amber and (ii) all modern ortholasmatines are restricted to East Asia and North and Central America.

Key words: Nemastomatidae, Ortholasmatinae, Baltic amber, Rovno amber, micro-CT, Priabonian, Eocene.

Christian Bartel [bartel@snsb.de; ORCID: http://orcid.org/0000-0003-2949-6890] (corresponding author), Naturkundemuseum Bamberg, Fleischstraße 2, 96047 Bamberg, Germany.
Plamen G. Mitov [pl_mitov@yahoo.com; ORCID: http://orcid.org/0000-0002-6191-4135], Department of Zoology and Anthropology, Faculty of Biology, Sofia University, 8 Dragan Zankov Blvd., 1164 Sofia, Bulgaria.
Jason A. Dunlop [jason.dunlop@mfn.berlin; ORCID: http://orcid.org/0000-0002-0179-6640], Museum für Naturkunde, Leibniz Institute for Evolution and Biodiversity Science, Invalidenstraße 43, 10115 Berlin, Germany.
Jörg U. Hammel [joerg.hammel@hereon.de; ORCID: http://orcid.org/0000-0002-6744-6811], Institute of Materials Physics, Helmholtz-Zentrum Hereon, Max-Planck-Straße 1, 21502 Geesthacht, Germany.

Received 28 August 2025, accepted 31 January 2026, published online 18 March 2026.

Introduction

Of the four living suborders of harvestmen (Arachnida: Opiliones), the Dyspnoi group represents the second smallest with just over 426 described species. Despite this relatively restricted number, as compared to the remaining about 6800 living harvestmen species, the group is morphologically diverse (Kury et al. 2024). While several dyspnoids are small, dark and rather inconspicuous, others have developed structures such as a highly modified eye tubercle, or hood such as is seen in the families Ceratolasmatidae, Dicranolasmatidae, Trogulidae and the subfamily Ortholasmatinae of the Nemastomatidae (Gruber 2007; see also below). All dyspnoids are characterized by a reduced or absent pedipalp claw and diaphanous teeth on the cheliceral fingers. Their modern biogeographic distribution is clearly focussed on the northern hemisphere (e.g., Schönhofer 2013).

The comparably low modern diversity of Dyspnoi is reflected in their fossil record. Thirteen fossils have been formally described, with four of the late Carboniferous age, belonging either to extinct families or unplaced at family level (e.g., Garwood et al. 2011; Kury et al. 2020). Another extinct family, Halithersidae, is known from mid-Cretaceous Burmese amber (Dunlop et al. 2016). There is a questionable shale-preserved Eocene record of the living genus *Trogulus* Latreille, 1802, from Geiselthal in Germany (Haupt 1956), while the remaining seven fossil dyspnoids all come from Eocene European ambers, i.e., Baltic, Bitterfeld, and Rovno. These include an extinct genus placed in the superfamily Ischyropsalidoidea (Dunlop et al. 2012), a member of the family Sabaconidae, and five species from the subfamily Nemastomatinae (e.g., Dunlop and Mitov 2009; Elsaka et al. 2019; Mitov et al. 2021 and references therein).

The subfamily Ortholasmatinae includes some of the most striking-looking modern harvestmen, as they often bear a very complex and branched ocular tubercle in combination with a unique dorsal micro-sculpture consisting of so-called keel cells (e.g., Shear and Gruber 1983; Shear 2010; Martens 2019). Seven extant genera with

27 described species are currently recognised with a disjunct distribution. *Asiolasma* Martens, 2019 (with 6 species) and *Cladolasma* Suzuki, 1963 (with 1 species) come from mainland Southeast Asia and Japan. *Cryptolasma* Cruz-López et al., 2018 (with 2 species), *Dendrolasma* Banks, 1894 (with 2 species), *Martensolasma* Shear, 2006 (with 2 species), *Ortholasma* Banks, 1894 (with 5 species) and *Trilasma* Goodnight & Goodnight, 1942 (with 9 species) all come from North America to Honduras. There are no modern representatives of this subfamily either in Europe or Central Asia. A Burmese amber dyspnoid fossil was initially placed in Ortholasmatinae, but (as noted above) this placement was questioned (Shear 2010) and it was subsequently transferred to a new family by Dunlop et al. (2016).

Here, we describe the first two unequivocal fossils of ortholasmatine harvestmen, which come from Eocene Baltic and Rovno amber dated to a still controversial Priabonian age of ca. 33.90–37.71 Ma (Iakovleva 2017; Dunlop et al. 2019; Mitov et al. 2021; and references therein). Given the often well-developed ocular process and dorsal ornamentation alluded to above, we applied for the first time high-resolution synchrotron-based computer tomography to a harvestman in amber, with the aim of facilitating better comparisons with the living genera and answering the question whether this European fossil has Asian or American affinities.

Nomenclatural acts.—This published work and the nomenclatural acts it contains have been registered in ZooBank: urn:lsid:zoobank.org:pub:BCECC013-3ED0-40CD-A810-650492B0F2E3

Institutional abbreviations.—MB.A., Museum Berlin, Arthropoda, Germany; MfN, Museum für Naturkunde, Berlin, Germany.

Other abbreviations.—ao, anal operculum; ch, chelicerae; cp, carapace process; cx, coxa; ey, eye lens; fe, femur; go, genital operculum; L, length; mt, metatarsus; oc, ocular tubercle; pa, patella; pp, pedipalp; ta, tarsus; ti, tibia; tr, trochanter; W, width.

Material and methods

The specimens studied here originate from the private collection of Jörg Wunderlich, Hirschberg–Leutershausen, Germany (the Baltic specimen) and Jonas Damzen, Vilnius, Lithuania (the Rovno specimen). Both fossils are now deposited in the Museum für Naturkunde Berlin (MB.A. 4454 and 4455). The Baltic specimen was photographed using a Zeiss Stereomicroscope Stemi 508 and a Zeiss Discovery V8. These takes a stack of images (20–50) at different focal planes which were combined into a single picture using Helicon Focus 7. Afterwards the picture was corrected for brightness and contrast using Photoshop CS5. The Rovno specimen was photographed by Jonas Damzen and we use these images with his permission. Interpretative drawings were made using a Leica M205C stereomicroscope with a camera lucida attachment. These were digitally redrawn following the methods of Coleman (2003) with Adobe Illustrator CS2 using a Wacom Intuos graphic tablet.

The synchrotron radiation based computer microtomography (SRμCT) scan of the male (Baltic specimen MB.A. 4454) was performed at the Imaging Beamline P05 (IBL) (Greving et al. 2014; Haibel et al. 2010; Wilde et al. 2016) operated by the Helmholtz-Zentrum Hereon at the storage ring PETRA III (Deutsches Elektronen Synchrotron DESY, Hamburg, Germany) using a photon energy of 18 keV and a sample to detector distance of 80 mm. Projections were recorded using a custom developed 20 MP CMOS camera system (Lytaev et al. 2014) with an effective pixel size of 1.27 μm. For each tomographic scan 2401 projections at equal intervals between 0 and π have been recorded. Tomographic reconstruction has been done by applying a transport of intensity phase retrieval and using the filtered back projection algorithm (FBP) implemented in a custom reconstruction pipeline (Moosmann et al. 2014) using Matlab (MathWorks) and the Astra Toolbox (Palenstijn et al. 2011; Van Aarle et al. 2015, 2016). Raw projections were binned two times for further processing, resulting in an effective pixel size of the reconstructed volume of 2.55 μm. VGSTUDIO MAX 3.4.3 was used to render and segment datasets at the Museum für Naturkunde, Berlin. Most of the important characters could be reconstructed using this method, except the male genitalia which are apparently not visible in the scan or not preserved. The Rovno specimen (MB.A. 4455) was not scanned due to its almost perfect preservation enabling detailed study by light microscopy.

The new fossils were compared with published descriptions of extant Ortholasmatinae harvestmen from the literature (Goodnight and Goodnight 1942; Suzuki 1963, 1974; Šilhavý 1973; Shear and Gruber 1983; Schwendinger and Gruber 1992; Shear 2006, 2010; Zhang and Zhang 2013; Cruz-López 2017; Cruz-López et al. 2018; Zhang et al. 2018; Martens 2019) (see also Introduction for further references).

All measurements are in mm and can represent slight approximations due to the three-dimensional position of the amber specimens in the amber matrix. Average values are marked with an asterisk (*). When the entire segment cannot be seen clearly and the measurement is incomplete, a plus (+) is added to the value.

Systematic palaeontology

Order Opiliones Sundevall, 1833

Suborder Dyspnoi Hansen & Sørensen, 1904

Family Nemastomatidae Simon, 1872

Subfamily Ortholasmatinae Shear & Gruber, 1983

Genus *Balticolasma* nov.

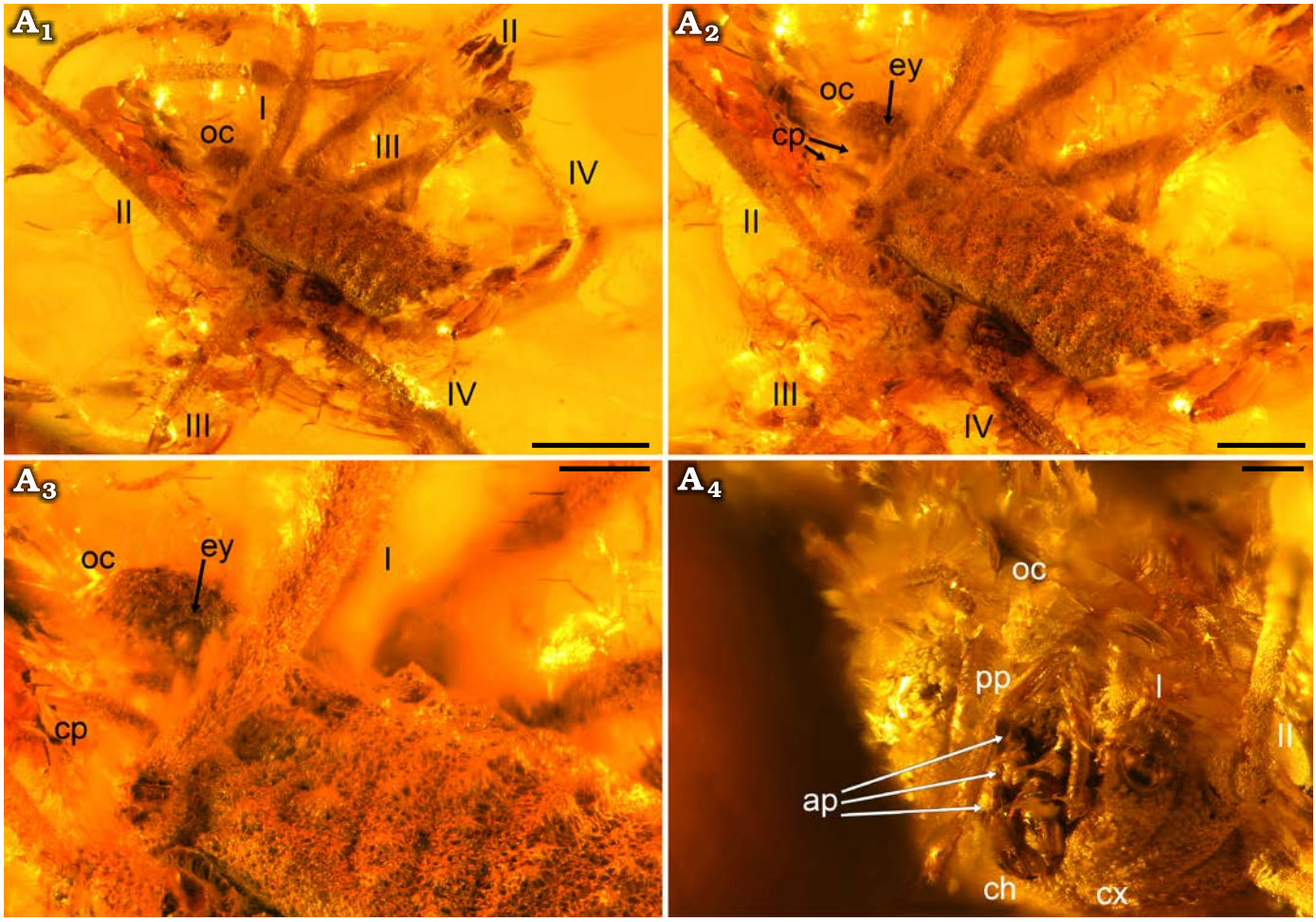

Fig. 1. Ortholasmatine harvestman *Balticolasma wunderlichi* gen. et sp. nov., holotype (male) MB.A.4454 from Baltic amber, 33.90–37.71 Ma, Priabonian. A_1, dorsolateral overview; A_2, close-up of the body (carapace processes and eye lens arrowed); A_3, close-up of the anterior body and ocular process; A_4, details of the chelicerae (apophyses arrowed). Abbreviations: ap, apophysis; ch, chelicerae; cp, carapace process; cx, coxa; ey, eye lens; oc, ocular tubercle; pp, pedipalp; legs numbered I–IV. Scale bars 1 mm (A_1), 0.5 mm (A_2) and 0.25 mm (A_3, A_4).

Type species: *Balticolasma wunderlichi* gen. et sp. nov.; by monotypy, see below.

Zoobank LSID: urn:lsid:zoobank.org:act:271C52E3-9023-4B95-8E43-E72465171531

Etymology: From the Baltic region where the amber hosting one of the specimens originates from and the suffix *lasma* applied to a few possibly closely related modern ortholasmatine genera.

Diagnosis.—As for the monotypic type species.

Remarks.—MB.A. 4454 is interpreted as a male, due to the presence of cheliceral apophyses. The missing pedipalp claw and a large ocularium extending anteriorly in the form of a hood strongly supports affinities to the Dyspnoi families Ceratolasmatidae, Dicranolasmatidae, Trogulidae, and Nemastomatidae (Ortholasmatinae). Of these, Trogulidae can be ruled out as the fossil bears cheliceral and pedipalpal apophyses (Figs. $1A_4$, $2A_2$, $3A_2$) and more than two tarsomeres on leg II. Dicranolasmatidae can also be excluded as their eyes are usually located on a bifurcating hood. The dorsal tuberculation (Figs. $1A_1$–A_3, $2A_1$, A_3, $3A_1$, A_3) of the fossil shows superficial similarities to certain genera of Ceratolasmatidae, particularly *Ceratolasma* Goodnight & Goodnight, 1942, redescribed and figured by Gruber (1978). However, the overall form and structure of the pedipalp and presence of pedipalp apophyses (Figs. $1A_4$, $3A_4$) argues against placement in this family. Furthermore, the hood in *Ceratolasma* is usually simple, nearly horizontal and extending in the form of a blunt club. The most similar condition to the fossil's ocular process can probably be found in the living ortholasmatine genus *Cryptolasma* from Mexico. However, the ocular process of the latter is much thinner, less curved and branched, i.e., ornate dorso-laterally with many, markedly elevated, anvil-shaped tubercles. A branched ocular process seems to be absent in the amber fossil as neither the CT scan nor light microscopy reveal such a feature (Figs. $1A_1$–A_3, $2A_1$, A_3, $3A_1$, A_3).

Most of the characters observed in the fossil are thus more consistent with members of the subfamily Ortholasmatinae such as the presence of cheliceral and pedipalpal apophyses, large lateral carapace processes, a flattened body and the hood; even though the appearance of the latter is

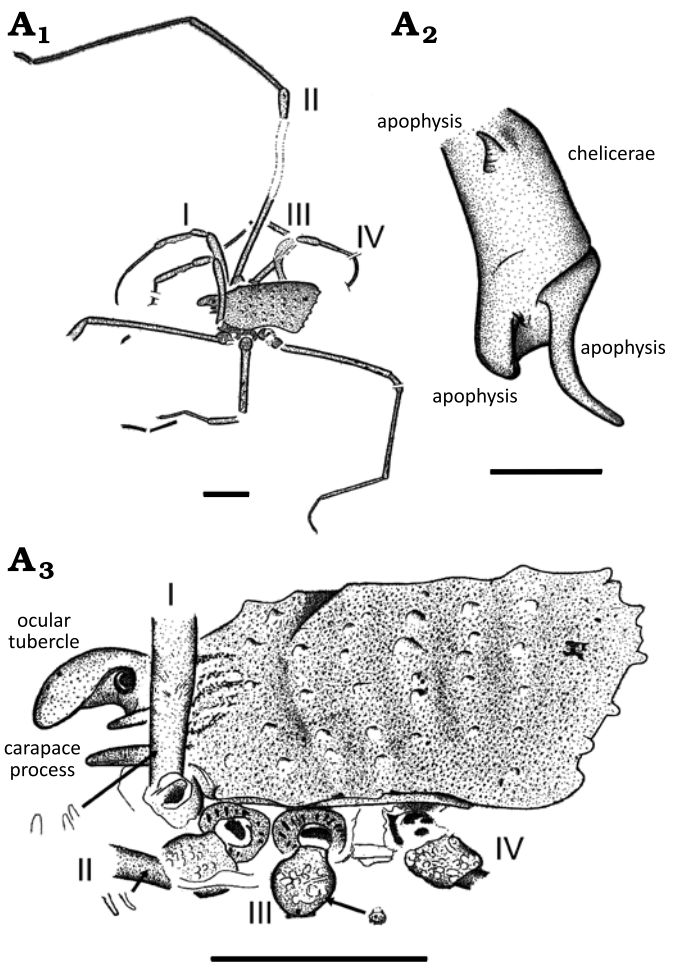

Fig. 2. Camera lucida drawings of ortholasmatine harvestman *Balticolasma wunderlichi* gen. et sp. nov., holotype (male) MB.A.4454 from Baltic amber, 33.90–37.71 Ma, Priabonian. A_1, body and legs in dorsolateral view; A_2, first segment of the left chelicera with apophyses in dorsal view; A_3, body in dorsolateral view. Arrows indicate the sculptural elements of leg femurs and trochanters. Legs numbered I–IV. Scale bars 1 mm (A_1, A_3) and 0.1 mm (A_2).

quite unique. Another important character for most modern Ortholasmatinae is the presence of dorsal keel-cells. Martens (2019) described a new Asian species *Asiolasma billsheari* Martens, 2019, with a very indistinct network of keel-cells, but these are not developed in the fossil. Martens (2019) further stated that Asian Ortholasmatinae are likely to represent a relict group indicated by plesiomorphic character states such as a poorly developed keel-cell network. We suggest that this new fossil may belong to the ancestral lineage for modern ortholasmatines and based on its unique character combinations the new fossil is placed in a new genus and species.

Stratigraphic and geographic range.—Baltic and Rovno ambers, Lutetian/Priabonian, Eocene, Paleogene.

Balticolasma wunderlichi gen. et sp. nov.

Figs. 1–7.

Zoobank LSID: urn:lsid:zoobank.org:act:7C1A6EBB-5850-4AE7-81F7-E681852D71D8

Etymology: In honour of Jörg Wunderlich (Hirschberg–Leutershausen, Germany) for his extensive work on amber spiders and who has continued to provide the authors with many interesting harvestman specimens. Name masculine and in genitive case.

Type material: Holotype, MB.A. 4454, relatively well preserved adult male with most important characters visible except ventral body. Paratype, MB.A. 4455, almost perfectly preserved female from Rovno amber (Ukraine, Rovno region; Paleogene, upper Eocene, Lutetian/Priabonian).

Type locality: Unknown locality in the Baltic Region.

Type horizon: Baltic amber, Lutetian/Priabonian, Eocene, Paleogene.

Material.—Type material only.

Diagnosis.— Relatively small (body length less than 3 mm, excluding the hood) ortholasmatine harvestman with a flattened body, dorsally with seven rows of prominent, distally increasing tubercles. Dorsal ornamentation in form of a complex, irregular fine weave composed of filamentous elements. Ocular process tuberculated in form of a large, arched, downwards-bending and unbranched hood extending anteriorly. Each side of the hood bears two differently sized digitiform processes projecting from the anterior margin of the prosoma. A third very small process is located below the largest process near coxa I. Chelicerae with three apophyses in males. First cheliceral segment with one dorsal conical apophysis proximally and an additional machete shaped apophysis distally. Second cheliceral segment with a long, downward curved sickle-shaped apophysis proximally. Pedipalps relatively short and slender. Pedipalp patella in males with rather small medio-distal spine-like apophysis. Legs long and somewhat granulated. Ventral body completely covered with rounded tubercles.

Description.—*Holotype*: MB.A. 4454, male, body small (L 2.16 mm, excluding the hood) and oval, flattened dorso-ventrally and dorsally with seven rows of tubercles increasing in size distally, prosoma W 0.92 mm, opisthosoma W 1.10 mm (Figs. $1A_1$–A_3, $2A_1$, A_3, $3A_1$, A_3). Tergites fused in a scutum magnum. Ocular process tuberculated and robust, extending anteriorly and forming a large, downwards-bending simple hood (L 0.89 mm; W 0.32 mm), bearing lateral eye lenses somewhat removed from the base; eye lens diameter 0.08 mm; the apical/distal part of the hood with visible holes/pores (Figs. $1A_3$, $2A_3$). Carapace with two lateral digitiform processes projecting anteriorly on each side, the outer one larger and longer (0.50 mm) than the inner one (0.18 mm) (Figs. $2A_1$, A_3, $3A_1$, A_3). A third very small digitiform process (visible frontally) is located below the largest process, near cx I.

Laminae chelicerales equivocal. Chelicerae relatively small and mostly smooth. The basal segment with a conical apophysis proximally and a machete-like apophysis distally (L 0.12 mm). Distal segment with a sickle-shaped and downwards bent apophysis proximally, L 0.17 mm; sparsely covered with small setae (Figs. $1A_4$, $2A_2$, $3A_2$). Chelicerae basal

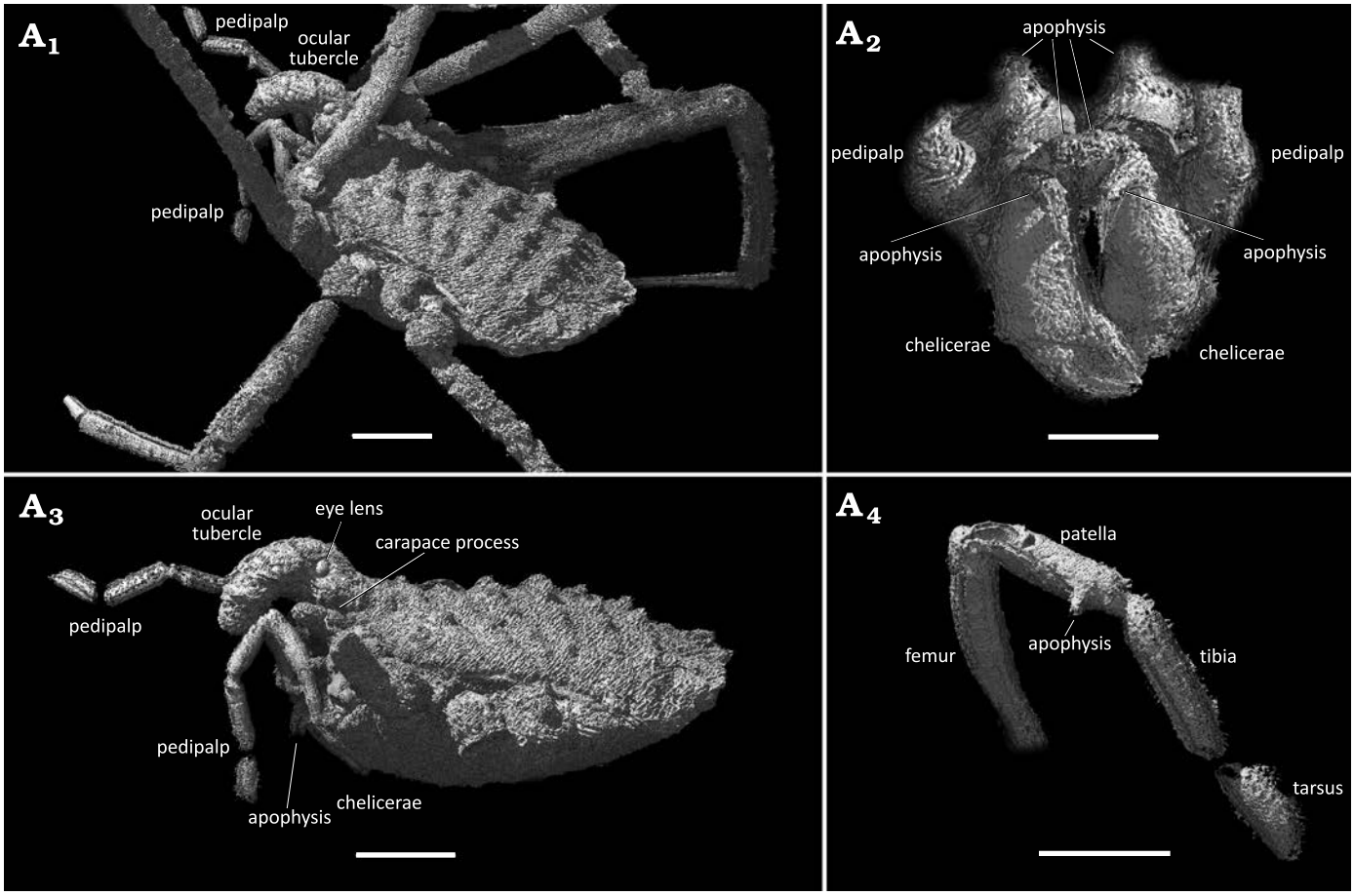

Fig. 3. 3D model of ortholasmatine harvestman *Balticolasma wunderlichi* gen. et sp. nov., holotype (male) MB.A.4454 from Baltic amber, 33.90–37.71 Ma, Priabonian. A_1, dorsolateral overview; A_2, details of the chelicerae, apophyses, frontal view; A_3, specimen without legs, eye lens and carapace process, lateral view; A_4, details of the left pedipalp, patella apophysis, dorso-mesal view. Legs numbered I–IV. Scale bars 0.5 mm (A_1, A_3); 0.2 mm (A_2) and 0.3 mm (A_4).

segment L c. 0.27 mm (+), distal segment L c. 0.57 mm, movable digit L 0.22 mm; fingers with black tips.

Pedipalps short, slender and covered with clavate setae on tibia and tarsus. Pedipalp tarsus especially setose. Pedipalp femur widens in its distal half, patella and tibia nearly cylindrical, patella with a small thorn-like apophysis medio-distally (Figs. $3A_4$, $4A_2$). Pedipalp claw absent. Pedipalp length: coxa and trochanter equivocal, fe 0.62* mm, pa 0.37* mm, ti 0.45* mm, ta 0.25 mm, total (fe–ta) 1.69 mm. Ratio ta/ti: 0.25/0.45 = 0.55.

Legs long and sometimes granulated. Leg II longest. Margins of leg coxae with anvil-shaped tubercles. Leg tarsi subdivided, ending in a single claw (L 0.10 mm). Metatarsus II with 8+ pseudoarticulations. Tarsal formula: 4–5; 6; 5; 5–6 (Fig. $4A_1$); Femur, patella I and III somewhat thickened. Femur I and III W 0.21. Ratio femur length/width (in dorsal view): I 1.37/0.21=6.52; II 2.70/0.175=15.43; III 1.34/0.21=6.38; IV 2.30/0.175=13.14. Leg length: Leg I cx 0.51 mm, tr 0.27* mm, fe 1.36* mm, pa 0.45 mm, ti .95* mm, mt 0.83 mm, ta 0.66 mm, total (cx–ta) 5.03 mm; Leg II cx 0.70 mm, tr 0.25* mm, fe 2.40* mm, pa 0.59* mm, ti 2.28* mm, mt 2.18* mm, ta 1.40* mm, total (cx–ta) 9.80 mm; Leg III cx 0.68 mm, tr 0.28* mm, fe 1.32* mm, pa 0.40* mm, ti 0.88* mm, mt 0.66* mm, ta 0.64* mm, total (cx–ta) 4.86 mm; Leg IV cx 0.63 mm, tr 0.28* mm, fe 2.07* mm, pa 0.47* mm, ti 1.81* mm, mt 1.32 mm, ta 0.79* mm, total (cx–ta) 7.37 mm.

Ventral characters equivocal.

Paratype: MB.A. 4455, female, body somewhat pear-shaped, flattened and again dorsally with seven rows of tubercles increasing in size distally, L 2.40 mm (excluding the hood), prosoma W 1.26 mm, opisthosoma W 1.69 mm (Fig. $5A_1$). Tergites fused in a scutum magnum. Last row of tubercles somewhat protruding the body posteriorly. Tuberculated ocular process robust, extending anteriorly and forming a large hood bending downwards (L 0.71 mm (+); W 0.47 mm), bearing lateral eye lenses near the middle, eye lens diameter 0.11 mm (Fig. $5A_2$). Carapace with additional lateral processes in form of digitiform spines, one larger (L 0.48 mm) and one smaller (at least 0.14 mm) closer to the hood on each side (Fig. $5A_1$, A_2), third processus not visible. Laminae chelicerales equivocal. Chelicerae relatively small and sparsely covered with small setae on the distal segment (Fig. $6A_1$, A_2). Cheliceral apophyses absent. Chelicerae basal segment equivocal L (?); distal segment L 0.45 mm, movable digit L 0.22 mm. Pedipalps short, slender and setose (clavate setae on tibia

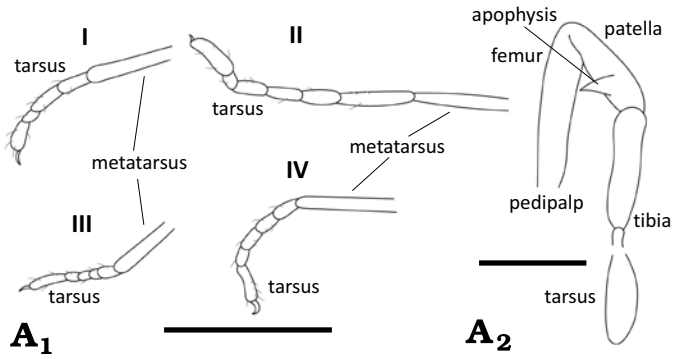

Fig. 4. Camera lucida drawings of ortholasmatine harvestman *Balticolasma wunderlichi* gen. et sp. nov., holotype (male) MB.A.4454 from Baltic amber, 33.90–37.71 Ma, Priabonian. A_1, leg tarsomeres; A_2, pedipalp without setae. Legs numbered I–IV. Scale bars 1 mm (A_1) and 0.25 mm (A_2).

and tarsus), especially on the tarsus (Fig. $6A_1$, A_2). Pedipalp patella apophysis and tarsal claw absent. Pedipalp length: tr 0.10 mm, fe 0.44 mm, pa (?), ti 0.20 mm(+), ta 0.19 mm, total (tr–ta, without pa) 0.93 mm. Legs long and granulated. Leg II longest. Leg coxae and trochanter almost completely tuberculated. Femur, patella I and III somewhat thickened. Leg tarsi subdivided, ending in a single claw. Metatarsus II with 8+ pseudoarticulations. Tarsal formula: 4–5; 8; 6; 6. Leg length: Leg I cx 0.59 mm, tr 0.19 mm, fe 0.12 mm, pa 0.48 mm, ti 0.84 mm, mt 0.64 mm, ta 0.60 mm, total (cx–ta) 4.46 mm; Leg II cx 0.63 mm, tr 0.23 mm, fe 2.80 mm, pa 0.56 mm, ti 2.48 mm, mt 2.20 mm, ta 1.16 mm, total (cx–ta) 10.06 mm; Leg III cx 0.61 mm, tr 0.21 mm, fe 1.20 mm, pa 0.37 mm, ti 0.60 mm, mt 0.88 mm, ta 0.84 mm, total (cx–ta) 4.71 mm; Leg IV cx 0.73 mm, tr 0.22 mm, fe 1.88 mm, pa 0.40 mm, ti 1.16 mm, mt 1.28 mm, ta 0.88 mm, total (cx–ta) 6.55 mm.

Ventral body completely covered with wart-like tubercles (Fig. $4A_1$, A_2). Genital operculum sub-trapezoidal and rounded anteriorly, L 0.86 mm, anterior W 0.40 mm, maximum posterior W 1.70 mm, with a subtle suture near the anterior margin. Anal operculum rounded L 0.43 mm, W 0.70 mm.

Remarks.—MB.A. 4455 (Figs. 5, 6) is interpreted as an adult female, as it lacks the apophysis on the cheliceral segments and on the pedipalp patella, and due to its relatively large size. Based on the similar habitus and ornament, it is fairly certain that this remarkably well-preserved specimen represents the same species as the Baltic amber male fossil described above. The massive, unbranched and downward-bending ocular process and the dorsal ornamentation are almost identical in the two specimens (Figs. 3 A_1–A_3, $5A_1$, A_2). Sexually dimorphic characters such as the already mentioned absence of cheliceral and pedipalpal apophyses and the larger size of the female can also often be observed in living nemastomatids and especially ortholasmatines (e.g., Shear and Gruber 1983; Shear 2010). In terms of leg length, the male fossil has proportionately slightly longer legs than the female. Some of the Recent species of the genera *Asiolasma*, *Cladolasma*, *Dendrolasma*, *Ortholasma*, and *Trilasma* also show a similar feature, or the length of the legs in both sexes is almost identical; while in other species of *Asiolasma*, *Ortholasma*, and *Trilasma* the females have much longer legs (see the data in Shear and Gruber 1983; Suzuki 1974; Shear 2010; Zhang et al. 2018; Martens 2019). The number of tarsomeres on the leg tarsi also differs somewhat in both fossils. Shear and Gruber (1983) already mentioned differences in the tarsal segment count, which is usually higher in males of Recent species on leg I and II. In our case, the female bears somewhat more tarsomeres. The number of tarsomeres on leg I and IV could be identical, however the exact number of tarsomeres remains difficult to resolve.

The almost perfect preservation of the Rovno fossil (MB.A. 4455) facilitates a closer look at the unusual dorsal ornamentation and it reveals further ventral details which could not be reconstructed in the Baltic specimen. As mentioned previously, living ortholasmatines are typically characterized by the presence of a distinct interconnected network of so-called keel cells dorsally, which consist of numerous anvil- and star-shaped tubercles. By contrast, the Rovno fossil shows a complex and irregular filamentous ornament with additional rows of tubercles, perhaps suggesting affinities with an early branch of the ortholasmatine lineage (Fig. $5A_1$). Some of the tubercles seem to be covered with a kind of secretion on their tips. Nevertheless, it remains uncertain whether these originate from the specimen or from the preservation. A tuberculated ventral body can also often be observed in modern ortholasmatines (e.g., Zhang and Zhang 2013).

Stratigraphic and geographic range.—In recent years the amber-bearing layer (Blue Earth) has been dated to a Priabonian age based on plant remains and dinoflagellate cysts (see e.g., Iakovleva 2017; Sadowski et al. 2017) instead of the previously proposed Lutetian. Baltic amber is distributed around the Baltic Sea region with the largest primary deposits in Kaliningrad and adjacent regions. Secondary, reworked occurrences are widespread in glacial and fluvial sediments throughout northern and central Europe. Rovno amber appears to be contemporaneous to Baltic amber based on stable isotope analyses performed in recent studies (e.g., Mänd et al. 2018). Therefore, it is also of Priabonian age and today primarily restricted to the northwestern Ukraine (Rovno region).

Discussion

Palaeobiogeography.—The new fossils (Fig. 7) indicate for the first time that harvestmen belonging to the subfamily Ortholasmatinae were also present in northern Europe during the late Eocene, but became extinct here at a later stage. It fits a broader geographical pattern in which Baltic and Rovno ambers sometimes preserve lineages which are now restricted to Asia and/or North America. Examples specifically relating to the harvestmen here would include the

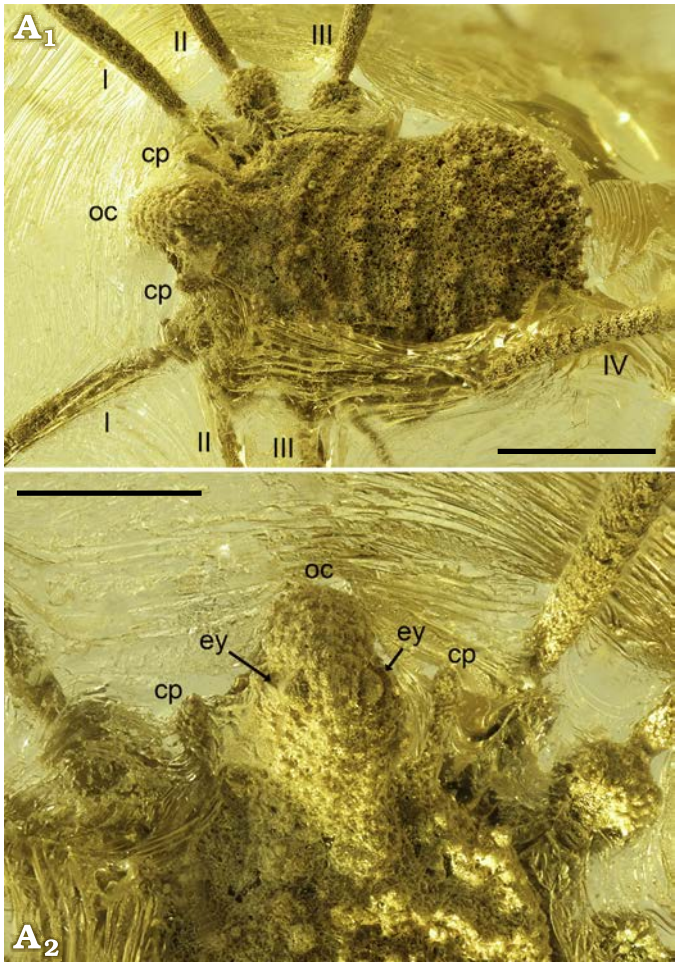

Fig. 5. Ortholasmatine harvestman *Balticolasma wunderlichi* gen. et sp. nov., paratype (female) MB.A.4455 from Rovno amber, 33.90–37.71 Ma, Priabonian. A_1, dorsal view of the body A_2, close-up of the ocular process in dorsal view, eye lenses arrowed. Abbreviations: cp, carapace process; ey, eye lens; oc, ocular process; legs numbered I–IV. Scale bars 1 mm (A_1) and 0.5 mm (A_2).

genera *Caddo* Banks, 1892, found today in Japan and North America and *Protolophus* Banks, 1893, and *Eumesosoma* Cokendolpher, 1980, both found in North America from the suborder Eupnoi (see Elsaka et al. 2019; Mitov et al. 2021). Also worth mentioning are *Sabacon* Simon, 1879, from the suborder Dyspnoi, found today in SW Europe, Asia, and North America (Elsaka et al. 2019; Mitov et al. 2021), and the amber species of *Siro* Latreille, 1797, from the suborder Cyphophthalmi (see discussions in Dunlop and Mitov 2011; and Karaman 2022 for *Neosiro* Newell, 1943).

Comparative remarks on extant Ortholasmatinae.—The new specimens express a specific combination of characters which cannot be exactly matched to any of the living ortholasmatines, and thus support the formation of a new genus. Unique to *B. wunderlichi* (albeit probably plesiomorphic) are: the dorsal sculpture, the type of hood, armament of the chelicerae and the number and shape of the apophyses. In the absence of data on the genitalia in fossils, we focus on taxonomically informative similarities from the body and appendages as compared to Recent ortholasmatine species.

Body: In both fossils the body is clean, i.e., it is not covered with dirt. From this we can assume that they probably led a more open and active lifestyle, perhaps living in an meso-xerophilic paleoenvironment (see below and also "Palaeoenvironment" in Mitov et al. 2021). At the same time, they do not appear to have developed glandular papillae, or else they are poorly developed or few in number, and any cutaneous secretion is weak. Absence of glandular papillae was interpreted by Shear and Gruber (1983: table 1) as a plesiomorphic ortholasmatine character.

Sculpture type: As noted above, a unique character of the new fossils, compared to other ortholasmatines, is the absence of keel-cells, branched tubercles, star-shaped tubercles and anvil-shaped tubercles; the latter only being present on the leg coxae of the fossil. In extant species these ornamentation types presumably have the function of combining mechanical strength and retention of both soil and moisture, similar to the condition observed in a number of Recent nemastomatines such as *Paranemastoma* spp., *Mitostoma* spp., *Carinostoma* spp., *Histricostoma* spp., *Mediostoma* spp., as well as the ortholasmatines, etc. These adaptations are thought to be necessary for living in moist to wet environments, with the need for a hydrophobic type of body surface and the easier removal of clay particles (see also Mitov 2011).

The dorsal body sculpture observed in the new fossils is unique. It is a combination of filamentous structures forming an irregular (mycelium-like) mesh, or structures resembling the wood pyre of logs, plus some tubercles (knobs-/buds-/lump-like), probably with a cleaning function (Figs. $1A_2$, $5A_1$). The dorsal body sculpture in these fossils may have conferred enough mechanical strength, but also lightness, under their specific living conditions. The fossils are also covered dorsally with seven rows of tubercles bearing rounded tips (blunt projections), which increase in size distally. In terms of these macrosculptural elements, the fossils bear similarities to some Asian and North American species. For example, in *Asiolasma angka* Schwendinger & Gruber, 1992 (Schwendinger and Gruber 1992: figs. 1, 3) the tubercles on the scutum show a similar shape and structure to those in the fossils. In *Asiolasma billsheari* Martens, 2019, areas I–IV of the opisthosoma each bear one pair of low pegs (Martens 2019: figs. 104–105). In *Cladolasma parvula* Suzuki, 1963 (Suzuki 1963: fig. 2; Suzuki 1974: fig. 1) the scutum is also armed with tubercles. In *Dendrolasma mirabile* Banks, 1894, the dorsum is armed with knobs (Shear and Gruber 1983: fig. 153). In *Ortholasma pictipes* Banks, 1911, and *O. levipes* Shear & Gruber, 1983, the dorsum is again armed with paired tubercles (spines/knobs) (Shear and Gruber 1983: figs. 4, 93, 94).

Ventrally, the fossils are covered with wart-like tubercles, which also cover the leg coxae. Wart-like tubercles further cover the hood, as well as the apophysis on both sides of the hood projecting from the anterior margin of the

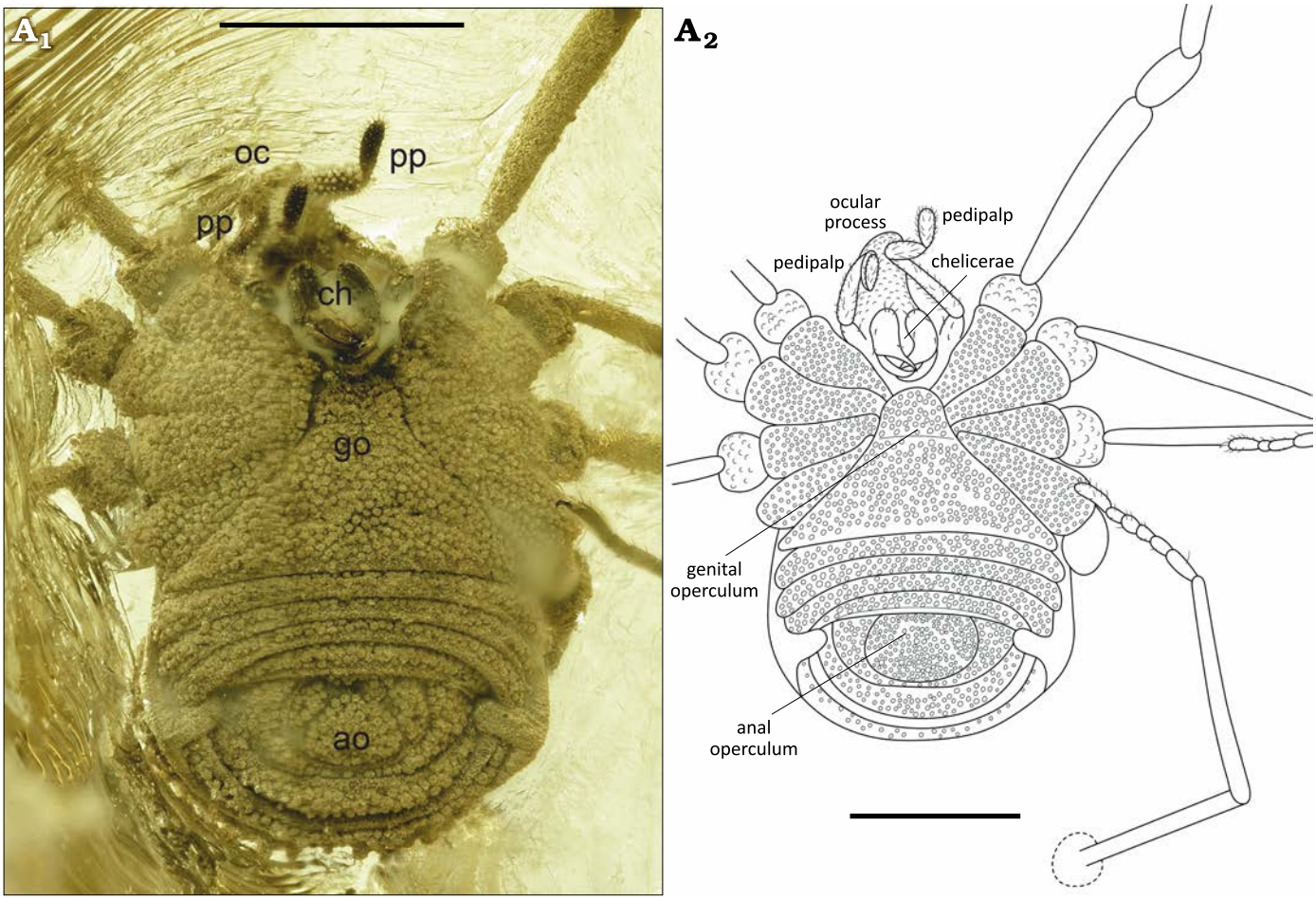

Fig. 6. Ortholasmatine harvestman *Balticolasma wunderlichi* gen. et sp. nov., paratype (female) MB.A.4455 from Rovno amber, 33.90–37.71 Ma, Priabonian. A_1, close-up of the ventral body; A_2, camera lucida drawing. Abbreviations: ao, anal operculum; ch, chelicerae; go, genital operculum; oc, ocular process; pp, pedipalp; legs numbered I–IV. Scale bars 1 mm.

prosoma. Similar to the fossils, tubercles and warts on the coxae and ventral side of the body are also present in some extant species, such as *Dendrolasma mirabile* (Shear and Gruber 1983: fig. 165), *Asiolasma ailaoshan* Zhang et al., 2018 (see in Zhang et al. 2018: figs. 1, 20). In *A. billsheari* the apophyses projecting from the anterior margin of the prosoma are also covered by small warts (Martens 2019: fig. 104).

Hood and prosomal processes: An open and active cursorial lifestyle in the fossils (see above) might also explain the shape and structure of the hood. This is not complex, as in some living species, but curves down and forms a more solid/compact structure. This may have protected the chelicerae and pedipalps during active locomotion, as well as retaining moisture and/or prey. We might speculate that this is either the plesiomorphic condition of the ortholasmatine hood, or that it could represent an adaptation to the environment and (micro)climate of the Baltic and Rovno amber forests during the late Eocene. However, determining the polarity of this character is contingent upon resolving relationships among the modern genera; compare alternative phylogenies in Shear and Gruber (1983), Cruz-López et al. (2018), and Martens (2019).

Generally, a more highly arched hood in modern species is characteristic of juveniles (Shear and Gruber 1983: 8), females and cave species. See, for example, Shear and Gruber (1983: figs. 124, 126) for *Ortholasma setulipes* Shear & Gruber, 1983, or Šilhavý (1973: fig. 146) for *Trilasma sbordonii* Šilhavý, 1973. Generally, when a more complex dorsal sculptural mesh is present on the body, the hood is more open and lattice-like, lighter, and probably also structurally stronger (compare Shear and Gruber 1983; Shear 2010).

In extant ortholasmatines it is noticeable that the more the hood is inclined and raised upwards (i.e., highly arched), and is narrower and/or longer, the more lateral processes/apophyses project from the anterior margin of the prosoma on each side. This arrangement may offer additional dorsal and fronto-lateral protection of the chelicerae and pedipalps when the animal is moving in tight spaces. For example, in species of *Ortholasma* (and some of *Trilasma*) the lateral processes on each side are two in number; in most *Trilasma* there are up to three, and in *Cryptolasma* there are four to five. By contrast, where the hood is flat

Fig. 7. Artistic reconstruction of the Eocene ortholasmatine harvestman *Balticolasma wunderlichi* gen. et sp. nov. (male) by Joshua Knüppe (Ibbenbüren, Germany).

and more horizontal (i.e., flat and more depressed), wide and spread out or fan-shaped (respectively relatively short), there is only one projection (in some species of *Asiolasma*, *Cladolasma*, *Dendrolasma*) or two lateral processes/apophyses (*Asiolasma angka*, *A. billsheari*, *A. juergengruberi* Martens, 2019). In such examples these are usually thick, with a blunt or slightly pointed tip (compare with Suzuki 1974; Shear and Gruber 1983; Shear 2010; Cruz-López et al. 2018; Martens 2019). In the complete absence of a developed hood (*Martensolasma*), there is only one short lateral process (compare Shear 2006; Cruz-López 2017).

The arrangement of the lateral processes (one short and one long) on both sides of the hood in the fossils is thus most similar to the condition in *Asiolasma* (Schwendinger and Gruber 1992: figs. 1–3; Martens 2019: figs. 18, 25, 64–66, 104), at least in terms of shape, position and number (Figs. $1A_2$, $2A_3$). The third, and smallest processus in the fossils is located lower down, below the long processus, similar to the condition in *Ortholasma* (Shear and Gruber 1983: figs. 21–29). Whether this small processus is in the process of development or in the process of reduction is difficult to say, but either way it demonstrates a primary condition of the character and the number of processes.

Chelicerae: The chelicerae of the male fossil have a total of three apophyses. Representatives of *Asiolasma* (*A. juergengruberi*, Martens 2019: fig. 72), *Dendrolasma*, *Martensolasma*, *Ortholasma rugosum* Banks, 1894, *Trilasma bolivari* Goodnight & Goodnight, 1942, *T. ranchonuevo* Shear, 2010, *T. tropicum* Shear, 2010, have a total of two. These consist of one tooth- or thorn-like apophysis on both the first (basal) article and on the second article of the chelicerae, where it can be horn- or sickle-like. In *Dendrolasma dentipalpe* Shear & Gruber, 1983, the first cheliceral segment has a large horn-like apophysis, which closely resembles the condition in *Balticolasma wunderlichi* gen. et sp. nov. Also, the second cheliceral segment additionally bears a massive apophysis, a large somewhat curved conical apophysis (Shear and Gruber 1983: figs. 192–193). In males of the remaining extant ortholasmatine species, only the second segment of the chelicerae bears a horn-like apophysis or curved tooth (*Cryptolasma aberrante* Cruz-López et al., 2018 and *C. citlaltepetl* Cruz-López et al., 2018). In the fossil the second cheliceral article bears

a strong horn- or sickle-like apophysis, but it appears to be closely related to the other species with a massively elevated apophysis on the second cheliceral article, namely the Asian species *A. ailaoshan*, *A. juergengruberi*, and *A. billsheari*. The proximal apophysis of the first cheliceral segment in *B. wunderlichi* could represent a gland opening, as it appears crater-like in the 3D model (Fig. $3A_2$).

Pedipalps: Like the pedipalps in the male fossil, the pedipalps of *Asiolasma* (*A. juergengruberi* and *A. billsheari*) and *Dendrolasma dentipalpe* also have a medio-distal hook- or thorn-like patellar apophysis (Shear and Gruber 1983; Martens 2019). It is interesting to note that the male pedipalps in *Balticolasma wunderlichi* gen. et sp. nov. are more slender, compared to those of modern species; a tendency also observed in other fossil nemastomatids (Dunlop and Mitov 2009: 355; Mitov et al. 2021: 61). In their shape the male pedipalps of the fossil resemble those of modern female ortholasmatines. It is untypical for males of extant species, where the female pedipalps are usually more slender. Males, by contrast, can have a highly developed (swollen, expanded) patella and tibia, probably as a result of the formation of more massive muscles for more leverage, or the formation of epigamic structures such as glandular fields and glandular organs.

Considering the multifunctionality of pedipalps and their morphotypes (see Wolff et al. 2016), the condition observed in modern ortholasmatines is probably the result of a specific selective pressure permitting limited opportunities to elongate their pedipalps hidden under the hood. This may relate to the changing climatic and ecological conditions (from the end of Eocene) under which the American and Asian populations of ortholasmatines evolved, and correspondingly to accompanying changes in terms of their trophic relationships such as the diversity of the food spectrum, the type, size, quality and agility of prey, and the prey capture mechanism used to secure the prey between the pedipalps (Wolff et al. 2016). Most likely, this modern morphotype is also a consequence of changes in behaviour and chemical communication related to reproduction: such as searching for the opposite sex under deteriorating, unfavourable conditions or narrow spaces, through chemical communication (reproductive tactics/epigamic sexual selection), and grasping and retention of the female during copulation (see Wolff et al. 2016), with the application of greater force than males in larger and heavier females, for example, in females of the genus *Ortholasma*. Usually glandular (or clavate) setae are numerous on the pedipalps of harvestmen living in environments with high humidity and feeding on small, agile prey, for example, in nemastomatids (see also Wolff et al. 2016). It is interesting to note that there are no clavate setae on the femora in the new fossil, and they are few and far between on the other segments of the pedipalps. This might imply that it inhabited drier habitats with a specific prey type, but still had the opportunity to catch and retain small Acari and Collembola when changing the (micro)habitat, while at the same time reducing the cost for the production of adhesive fluid. Like the fossil, the Recent *Dendrolasma dentipalpe*, *Asiolasma angka*, *A. billsheari*, and *A. juergengruberi* lack clavate setae on the palpal femora (Shear and Gruber 1983: fig. 194; Martens 2019: figs. 29–30, 67–68, 71, 115), as this part of the limb is probably not involved in the retention of prey items.

Leg ornamentation: In the new fossil, only the leg coxae bear anvil-shaped tubercles, similar in type to those of modern species (Shear and Gruber 1983; Schwendinger and Gruber 1992; Shear 2010; Zhang and Zhang 2013; Cruz-López et al. 2018; Zhang et al. 2018; Martens 2019). Additionally, the leg trochanters of the fossils are more spherical in shape and densely covered with a nodular or knobbly sculpture composed of wart-like tubercles (Fig. $2A_3$: arrows). There are similar macrosculptural elements on the trochanters of the legs in, e.g., *Asiolasma ailaoshan* (Zhang et al. 2018: fig. 5) and *Dendrolasma mirabile* (Shear and Gruber 1983: fig. 164), but they are not so densely arranged.

The femoral microsculpture of the fossils (Fig. $2A_3$: arrows) consists of uniform and evenly scattered blunt, conical denticles with rounded tips, which are only slightly compressed. They are similar in type to those on the leg femora of some species of *Ortholasma*; for example, *O. pictipes*, *O. rugosum*, *O. levipes* (see Shear and Gruber 1983: figs. 18, 47, 104), and *O. colossus* Shear, 2010 (Shear 2010: fig. 7).

Leg II metatarsus pseudoarticulations: A potentially primitive character are the pseudoarticulations on Mt II. They are already present in earlier instars (Shear and Gruber, 1983) and can be found in most species of ortholasmatines (Suzuki 1974; Shear and Gruber 1983; Shear 2010; Cruz-López 2017; Cruz-López et al. 2018), including the new fossils. In extant species they usually vary from 2 to 12. *Balticolasma wunderlichi* gen. et sp. nov. bears at least 8 pseudoarticulations on Mt II. The extant species *Ortholasma rugosum* (with 7), *O. pictipes* (with 9), *Trilasma sbordonii* (with 7), and *T. petersprousei* Shear, 2010 (with 12) have a comparable number of pseudoarticulations as the fossils.

Affinities and zoogeographical comments.—A key question is whether the affinities of the new fossils lie with the modern East Asian or American faunas? This also relates to the wider, and still not satisfactorily resolved, question of where Ortholasmatinae originated. Shear (2010) entertained origins in the New World, but Martens (2019) suggested several lines of evidence for an Asian origin, with the American species being more derived. Alternatively, the phylogenetic analysis of Cruz-López et al. (2018: figs. 1, 2) recovered their new Mexican genus *Cryptolasma* as the sister-group of the remaining ortholasmatines, which could be consistent with a scenario in which the subfamily originated in Central America and subsequently spread into North America and Asia. The genital characters and ecological arguments, i.e., American species have more complex male genitalia and

occupy a more diverse range of habitats, cannot be tested in the fossils, due to the lack of sufficient information.

From the comparisons above, it is clear that the amber fossils show features seen in both extant Asian (*Asiolasma*, *Cladolasma*) and American (*Dendrolasma*, *Martensolasma*, *Ortholasma*, and *Trilasma*) genera, but *Balticolasma wunderlichi* gen. et sp. nov. appears, on balance, to be closer to the Asian species albeit with most of its characters in an even more simplified condition. The ocular process of the fossil is more robust, but only covered with smaller tubercles, and the dorsal body ornamentation lacks any particular pattern of keel cells, branched tubercles, or star- and anvil-shaped tubercles (except on the leg coxae). Martens (2019) noted that Asian taxa tend to have a more irregular dorsal ornamentation, less clearly organised into discrete cells. Furthermore, the hood in Asian species has lateral tubercles which are free along their length while the hood of many American species is more complex with interlinking elements between the lateral tubercles to produce a net- or lattice-like morphology, arguably conferring more stability.

These observations could lend weight to Martens (2019) proposal that ortholasmatines first evolved in the Old World. We might even speculate that the group originated in the western Palaearctic, where it was represented by less morphologically derived lineages, even though it eventually became extinct here. The greater morphological similarity between the amber fossils and the modern Asian ortholasmatines could favour an older, closer, relationship between the Old World ortholasmatines. This still needs to be reconciled with the molecular data underlying the phylogeny proposed by Cruz-López et al. (2018) where the Neotropical taxa emerged as the basal group.

We should, however, also note that Martens (2019: 108) stated that Asian ortholasmatines preferably "…live in humid litter or under pieces of dead wood in primeval forests, montane broadleaf forests, coniferous forests and (sub) tropical evergreen forests, with a closed canopy". Habitats like this were not so clearly present in the probably humid but warm-temperate climate of the Baltic amber forests, according to Sadowski et al. (2017) and the Rovno amber forests (Mitov et al. 2021 and literature therein). However, extant floras (based on conifers) which come closest in representing the Baltic amber forests can be found today in East Asia (especially south-eastern China) and North America including Mexico (Sadowski et al. 2017: table 12). Both areas are today still inhabited by a few of the Asian and most of the American ortholasmatines respectively. A western Palaearctic origin for ortholasmatines would also be consistent with the concentrated high diversity of the second nemastomatid subfamily (and putative sister-group), Nemastomatinae, in this region.

The first European ortholasmatine is nevertheless particularly significant in biogeographical terms, as it finally fills the disjunct gap between East Asian and North American populations seen today. These disjunct distribution patterns usually imply an ancient, and relictual, nature for a given organism group. An alternative example would be horseshoe crabs (Lamsdell 2020: fig. 2), which are nearshore marine rather than terrestrial but are also only found today in East Asia and along the eastern coast of North America.

This prompts us to consider a third scenario for ortholasmatine origins which may be able to unify the historical biogeography hypothese proposed by Shear and Gruber (1983) and Martens (2019). We suggest that ortholasmatines could be an old and relictual group, which were probably much more widespread in the past with populations occupying more extensive ranges in Eurasia, or indeed the entire Holarctic. Connections between these populations were old, most likely Laurasian, and might even date back to the Triassic (ca. 200 Myr) before the opening of the present Atlantic Ocean (see also Shear and Gruber 1983; discussion in Dunlop and Mitov 2011). The disjunction between the American and Asian ortholasmatines is most likely the result of paleogeographic and climatic changes that began long before the Pleistocene. These changes may be related to long term global cooling and increasing continentality of the climate, as well as subsequent dramatic events during glacial times. These changes may have led to fragmentation and isolation of ortholasmatine populations. In our model, a large part of the hygrophilous and thermophilous forms (including the amber fossils described herein) died out, probably as a result of aridification and/or the loss of Eurasian Forest communities and steppefication of the landscape.

In this scenario, a consequence of this was that the European Ortholasmatinae taxa disappeared, while the more ecologically plastic American and Asian species were able to migrate southwards, along with the rest of the terrestrial invertebrate biota. Later, through the spread of forest formations during interglacial and postglacial expansion, they were able to migrate back northward in the opposite direction. Perhaps they were able to survive adverse periods in Holarctic refugia, varying in number, type and variety. Under certain conditions, American and Asian ortholasmatines may also have had the opportunity for intercontinental exchange, probably across a humid Bering land bridge during the early Cenozoic (see also Shear and Gruber 1983). As a result of the gradual adaptation to the specific local ecological conditions in a cold and cool climate (since the end of the Eocene–Oligocene), a number of psychrophilous and frigostable species associated with both humid environments and drier habitats have appeared. Their descendants now inhabit the territory of the American and Asian continents, mainly within relict plant communities and under relict climatic conditions (see Shear and Gruber 1983: 13; Martens 2019: 108–109).

Conclusions

The first ortholasmatine fossils come from Eocene Baltic and Rovno amber and improve our understanding of the evolutionary history of this unique group of harvestmen.

Baltic amber inclusions are already known for their great diversity and continue to reveal species which are not present in Europe today. The additional specimen from Rovno amber shows again that both amber sources share a common harvestmen fauna and are thus probably of contemporary Eocene age. With the new material, the number of known Baltic and Rovno amber harvestmen species become 19 and seven, respectively, and the number of species common to both faunas is now six (see also Mitov et al. 2021: table 1). Our new fossils also represent the first unequivocal calibration point for Ortholasmatinae, which can be used in future studies to date the harvestman tree of life more precisely. However, many questions remain, and additional fossil finds from other sources would be necessary to fully reconstruct the history of Ortholasmatinae.

Acknowledgements

First of all, we want to thank Jörg Wunderlich (Hirschberg-Leutershausen, Germany) and Jonas Damzen (Vilnius, Lithuania) for making the specimens described here available. We acknowledge provision of beamtime, related to the proposal BAG-20190010 at beamline P05 at PETRA III at DESY, a member of the Helmholtz Association, Germany. We acknowledge the support during the beam time by Fabian Wilde, Julian Moosmann, and Felix Beckmann (all Deutsches Elektron-Synchrotron DESY, Hamburg, Germany). This research was supported in part through the Maxwell computational resources operated at Deutsches Elektronen-Synchrotron DESY, Hamburg, Germany. In addition, we want to thank Kristin Mahlow and Simon Beurel (both MfN) for technical support during the creation of the 3D model. Pavel E. Tarasov (Freie Universität Berlin, Germany) and two anonymous reviewers provided helpful comments on an earlier version of the manuscript. CB was supported by an Elsa-Neumann Scholarship from the Freie Universität, Berlin. PGM visited to Museum für Naturkunde Berlin supported by the SYNTHESYS project (http://www.synthesys.info/), financed by the European Community Research Infrastructure Action under the FP7 ‘Capacities’ Programme (DE-TAF-4010).

Editor: Krzysztof Hryniewicz

References

Banks, N. 1892. A new genus of Phalangiidae. *Proceedings of the Entomological Society of Washington* 2: 249–250.

Banks, N. 1893. The Phalanginae of the United States. *The Canadian Entomologist* 25: 205–211.

Banks, N. 1894. The Nemastomatidae and Trogulidae of the United States. *Psyche* 7: 11–12.

Banks, N. 1911. The Phalangida of California. *Pomona College Journal of Entomology, Claremont* 3: 412–421.

Cokendolpher, J.C. 1980. Replacement name for *Mesosoma* Weed, 1892 with a revision of the genus (Opiliones, Phalangiidae, Leiobuninae). *Occasional Papers, Museum of Texas Tech University* 66: 1–19.

Coleman, C.O. 2003. “Digital inking”: How to make perfect line drawings on computers. *Organism, Diversity and Evolution, Electronic Supplement* 14: 1–14. [http://senckenberg.de/odes/03-14.htm].

Cruz-López, J.A. 2017. A second species of the genus *Martensolasma* (Opiliones, Dyspnoi, Nemastomatidae) from Mexico. *Zootaxa* 4338: 526–532.

Cruz-López, J.A., Cruz-Bonilla, A., and Francke, O.F. 2018. Molecules and morphology reveal a new aberrant harvestman genus of Ortholasmatinae (Opiliones, Dypsnoi, Nemastomatidae) from Mexico. *Systematics and Biodiversity* 16: 714–729.

Dunlop, J.A. and Mitov, P.G. 2009. Fossil harvestmen (Arachnida, Opiliones) from Bitterfeld amber. *In*: P. Stoev, J.A. Dunlop, and S. Lazarov (eds.), A life caught in a spider’s web. Papers in arachnology in honour of Christo Deltshev. *ZooKeys* 16: 347–375.

Dunlop, J.A. and Mitov, P.G. 2011. The first fossil cyphophthalmid (Opiliones) from Baltic amber. *Arachnologische Mitteilungen* 40: 47–54.

Dunlop, J.A., Bartel, C., and Mitov, P.G. 2012. An enigmatic spiny harvestman from Baltic amber. *Fossil Record* 15: 91–101.

Dunlop, J.A., Selden, P.A, and Giribet, G. 2016. Penis morphology in a Burmese amber harvestman. *The Science of Nature* 103: 1–5.

Dunlop, J.A., Vlaskin, A.P., and Marusik, Y. 2019. Comparing arachnids in Rovno amber with the Baltic and Bitterfeld deposits. *Paleontological Journal* 53: 1074–1083.

Elsaka, M., Mitov, P.G., and Dunlop, J.A. 2019. New fossil harvestmen (Arachnida: Opiliones) in the Hoffeins amber collection. *Neues Jahrbuch für Geologie und Paläontologie Abhandlungen* 292: 155–169.

Garwood, R.J., Dunlop, J.A., Giribet, G., and Sutton, M.D. 2011. Anatomically modern Carboniferous harvestmen demonstrate early cladogenesis and stasis in Opiliones. *Nature Communications* 2: 1–7.

Goodnight, C.J. and Goodnight, M.L. 1942. New American Phalangida. *American Museum Novitates* 1211: 1–18.

Greving, I., Wilde, F., Ogurreck, M., Herzen, J., Hammel, J.U., Hipp, A., Friedrich, F., Lottermoser, L., Dose, T., Burmester, H., Müller, M., and Beckmann, F. 2014. P05 imaging beamline at PETRA III: First results. *In*: J. Moosmann, A. Ershov, V. Weinhardt, T. Baumbach, M.S. Prasad, C. LaBonne, X. Xiao, J. Kashef, and R. Hoffmann (eds.), *Developments in X-ray Tomography IX. Proceedings of SPIE 9212*, 92120O. SPIE, Bellingham.

Gruber, J. 1978. Redescription of *Ceratolasma tricantha* Goodnight & Goodnight, with notes on the family Ischyropsalidae (Opiliones, Palpatores). *Journal of Arachnology* 6: 105–124.

Gruber, J. 2007. Nemastomatidae. *In*: R. Pinto da Rocha, G. Machado, and G. Giribet (eds.), *Harvestmen. The Biology of Opiliones*, 148–151. Harvard University Press, Cambridge.

Haibel, A., Beckmann, F., Dose, T., Herzen, J., Ogurreck, M., Müller, M., and Schreyer, A. 2010. Latest developments in microtomography and nanotomography at PETRA III. *Powder Diffraction* 25: 161–164.

Hansen, H.J. and Sørensen, W. 1904. *On Two Orders of Arachnida*. 178 pp. Cambridge University Press, Cambridge.

Haupt, H. 1956. Beitrag zur Kenntnis der eozänen Arthropodenfauna des Geiselthals. *Nova Acta Leopoldina (new series)* 128: 1–90.

Iakovleva, A.I. 2017. Detalization of Eocene dinocyst zonation for Eastern Peritethys. *Bjulleten' Moskovskogo obŝestva ispytatelej prirody. Otdel geologičeskij* 92: 32–48. [In Russian, with English summary]

Karaman, I. 2022. North American sironids (Opiliones, Cyphophthalmi) and composition of the family Sironidae with a description of two new species. *Biologia Serbica* 44: 51–77.

Kury, A.B., Dunlop, J.A., and Mendes, A.M. 2020. On the allocation of some Palaeozoic and Tertiary harvestmen. *In*: A.B. Kury, A.C. Mendes, L. Cardoso, M.S. Kury, and A.A. Granado (eds.), *WCO-Lite: Online World Catalogue of Harvestmen (Arachnida, Opiliones). Checklist of All Valid Nomina in Opiliones with Authors and Dates of Publication up to 2018*, 49–51. Self-published, Rio de Janeiro.

Kury, A.B., Mendes, A.C., Cardoso, L., Kury, M.S., Granado, A.de A., Giribet, G., Cruz-López, J.A., Longhorn, S.J., Medrano, M., Oliveira, A.B.R. de, Kury, I.S., and Souza-Kury, M.A. 2024. *World Catalogue of Opiliones. WCO-Lite version 2.7*. https://wcolite.com/ (accessed 12 June 2025).

Lamsdell, J.C. 2020. The phylogeny and systematics of Xiphosura. *PeerJ* 8: e10431.

Latreille, P.A. 1797. *Précis des caractères génériques des insectes, disposés dans un ordre naturel*. 113 pp. Prévot, Paris.

Latreille, P.A. 1802. *Histoire naturelle, générale et particulière des crustacés et des insectes. Familles naturelles des genres. Tome troisième*. 467 pp. F. Dufart, Paris.

Lytaev, P., Hipp, A., Lottermoser, L., Herzen, J., Greving, I., Khokhriakov, I., Meyer-Loges, S., Plewka, J., Burmester, J., Caselle, M., Vogelgesang, M., Chilingaryan, S., Kopmann, A., Balzer, M., Schreyer, A., and Beckmann, F. 2014. Characterization of the CCD and CMOS cameras for grating-based phase-contrast tomography. *Proceedings of SPIE* 9212: 921218.

Mänd, K., Muehlenbachs, K., McKellar, R.C., Wolfe, A.P., and Konhauser, K.O. 2018. Distinct origins for Rovno and Baltic ambers: Evidence from carbon and hydrogen stable isotopes. *Palaeogeography, Palaeoclimatology, Palaeoecology* 505: 265–273.

Martens, J. 2019. An ancient radiation: Ortholasmatine harvestmen in Asia—a new genus, three new species and a revision of the known species (Arachnida, Opiliones, Nemastomatidae). *Revue Suisse de Zoologie* 126: 79–110.

Mitov, P.G. 2011. A new anophthalmous species of *Paranemastoma* from Bulgaria (Opiliones: Nemastomatidae). *Journal of Arachnology* 39: 303–319.

Mitov, P.G., Perkovsky, E.E., and Dunlop, J.A. 2021. Harvestmen (Arachnida: Opiliones) in Eocene Rovno amber (Ukraine). *Zootaxa* 4984: 43–72.

Moosmann, J., Ershov, A., Weinhardt, V., Baumbach, T., Prasad, M.S., LaBonne, C., Xiao, X., Kashef, J., and Hofmann, R. 2014. Time-lapse X-ray phase-contrast microtomography for in vivo imaging and analysis of morphogenesis. *Nature Protocols* 9: 294–304.

Newell, I.M. 1943. A new sironid from North America (Opiliones, Cyphophthalmi, Sironidae). *Transactions of the American Microscopical Society* 62: 416–422.

Palenstijn, W.J., Batenburg, K.J., and Sijbers, J. 2011. Performance improvements for iterative electron tomography reconstruction using graphics processing units (GPUs). *Journal of Structural Biology* 176: 250–253.

Sadowski, E.M., Schmidt, A.R., Seyfullah, L.J., and Kunzmann, L. 2017. Conifers of the "Baltic amber forest" and their palaeoecological significance. *Stapfia* 106: 1–73.

Schönhofer, A. 2013. A taxonomic catalogue of the Dyspnoi Hansen and Sørensen, 1904 (Arachnida: Opiliones). *Zootaxa* 3679: 1–68.

Shear, W.A. 2006. *Martensolasma jocheni*, a new genus and species of harvestman from Mexico (Opiliones, Nemastomatidae, Ortholasmatinae). *Zootaxa* 1325: 191–198.

Shear, W.A. 2010. New species and records of ortholasmatine harvestmen from México, Honduras, and the western United States (Opiliones, Nemastomatidae, Ortholasmatinae). *ZooKeys* 52: 9–45.

Shear, W.A. and Gruber, J. 1983. The opilionid subfamily Ortholasmatinae (Opiliones, Troguloidea, Nemastomatidae). *American Museum Novitates* 2757: 1–65.

Simon, E. 1872. Notices sur les arachnides cavernicoles et hypogés. *Annales de la Société Entomologique de France* 5: 214–244.

Simon, E. 1879. *Les Arachnides de France*. *Tome 7. Contenant les ordres des Chernetes, Scorpiones et Opiliones.* 332 pp. Librairie Encyclopédique de Roret, Paris.

Šilhavý, V. 1973. Cavernicolous opilionids from Mexico (Arachnida: Opiliones). Part II. *Accademia Nazionale dei Lincei, Problemi Attualli di Scienza e di Cultura* 171: 175–194.

Sundevall, C.J. 1833. *Conspectus Arachnidum*. 39 pp. C.F. Berling, Lund.

Suzuki, S. 1963. *Cladolasma parvula*, gen. et sp. nov. (Trogulidae: Opiliones) from Japan. *Annotationes zoologicae japonenses* 36: 40–43.

Suzuki, S. 1974. Redescription of *Dendrolasma parvula* (Suzuki) from Japan (Arachnida, Opiliones, Dyspnoi). *Journal of Science of Hiroshima Universi*ty 25: 83–108.

Schwendinger, P.J. and Gruber, J. 1992. A new *Dendrolasma* (Opiliones, Nemastomatidae) from Thailand. *Bulletin of the British Arachnological Society* 9: 57–60.

Wilde, F., Ogurreck, M., Greving, I., Hammel, J.U., Beckmann, F., Hipp, A., Lottermoser, L., Khokhriakov, I., Lytaev, P., Dose, T., Burmester, H., Müller, M., and Schreyer, A. 2016. Micro-CT at the imaging beamline P05 at Petra III. *AIP Conference Proceedings* 1741: 030035-1–4.

Wolff, J.O., Schönhofer, A.L., Martens, J., Wijnhoven, H., Taylor, C.K., and Gorb, S.N. 2016. The evolution of pedipalps and glandular hairs as predatory devices in harvestmen (Arachnida, Opiliones). *Zoological Journal of the Linnean Society* 177: 477–695.

Van Aarle, W., Palenstijn, W.J., Cant, J., Janssens, E., Bleichrodt, F., Dabravolski, A., De Beenhouwer, J., Batenburg, K.J., and Sijbers, J. 2016. Fast and flexible X-ray tomography using the ASTRA Toolbox. *Optics Express* 24: 25129–25147.

Van Aarle, W., Palenstijn, W.J., De Beenhouwer, J., Altantzis, T., Bals, S., Batenburg, K.J., and Sijbers, J. 2015. The ASTRA Toolbox: A platform for advanced algorithm development in electron tomography. *Ultramicroscopy* 157: 35–47.

Zhang, C. and Zhang, F. 2013. Description of a new *Cladolasma* (Opiliones: Nemastomatidae: Ortholasmatinae) species from China. *Zootaxa* 3691: 443–452.

Zhang, F., Zhao, L., and Zhang, C. 2018. *Cladolasma ailaoshan*, a new species of the genus *Cladolasma* Suzuki, 1963 from China (Opiliones, Nemastomatidae, Ortholasmatinae). *ZooKeys* 748: 11–20.